UNIVERSITY OF COLORADO BOULDER

HONORS THESIS - DEPARTMENT OF PHYSICS

Ultra-low Phase Noise Microwave Measurement

Author:
Romeo PETRIC

Thesis advisor:
Dr. Thomas SCHIBLI

Thesis committee:
Thomas Schibli and John Cumulat, Department of Physics
and Sebastian Casalaina-Martin, Department of Mathematics

April 3, 2023

UNIVERSITY OF COLORADO BOULDER

Abstract

Thomas Schibli

Department of Physics

Bachelor of Arts

Ultra-low Phase Noise Microwave Measurement

by Romeo PETRIC

Recent advancements in laser technology has enabled the generation of ultra-low phase noise microwaves. These highly stable signals are of great interests for their applications in communications, radars, and astronomy. The low loss of optical components, such as optical cavities and optical fibers, offer a high quality factor, which is essential to obtain a low phase noise. Ultra-short pulses of light emitted by mode-locked lasers at very high frequencies can be photo-detected to transfer their stability to the microwave domain. The stability of these pulse trains is achieved by locking an optical frequency comb to an optical cavity. The complexity and the size of these systems limit their applications to laboratories. A specific kind of laser called the monolithic mode-locked laser emits highly stable pulse trains with an ultra-low noise, and without the need for bulky stabilization setups. In this thesis, we measure the phase noise of a 16 GHz microwave generated by the monolithic mode locked laser. To measure such a low phase noise, a stabilized optical frequency comb will be used as optical reference. The microwave signal and the reference comb will be compared using dual output Mach-Zehnder modulators. The noise of the measurement setup will be diminished using a two channel cross-correlation technique. We will find that the monolithic mode lock laser can reach phase noise levels lower than the best compact microwave sources.

Contents

List of Figures

List of Tables

Chapter 1

Introduction

Electromagnetism not only changed our conception of electricity and magnetism, it also set a technological revolution through the discovery of electromagnetic waves. In 1901, the use of low frequency electromagnetic waves, known as radio waves, have permitted the very first wireless communication across the Atlantic [1]. Higher radio frequencies (RF) called microwaves were also investigated, but their limitation to line of sight paths led to the development of radio technology. The practical use of microwaves emerged before and during World War II with radars. Thanks to their large information carrying capacity, microwave signals were then used in communication systems, for phone calls and television distribution. The rapid growth of microwave-based technologies came with the demand for higher quality signals. Low quality signals are said to be noisy, they lead to errors in signal processing and consequently to altered messages. The quest for low noise microwaves is importantly driven by the search for highly performant radars. The invention of stealth aircrafts is an example for the motivation to generate ultra-low noise microwaves. A noisy microwave source can mask the return signal of a moving object. The echo from the environment results in radar clutter and may hide a target, which will thus go undetected. Many more technological and scientific applications are of interests. Microwaves are used in astronomy, to study celestial objects and map the universe. A recent achievement is the first image of a black hole using very long baseline interferometry. This method of observation requires very stable reference signals to properly synchronize the different antennas. Fluctuations in the phase of a signal, i.e. phase noise, impedes with the accuracy of the measurement and results in lower resolution images. Minimizing phase noise improves resolution in other imaging

techniques making use of microwaves, medical imaging being an example. More generally, lower phase noise will benefit communication and measurement systems. Phase noise is central in setting the performance limit of these timing-sensitive systems. Ultra-stable microwave signals are crucial in providing a good timing reference for data modulation. With an ultra-low phase noise signal used as a clock, the sampling rate for analog to digital conversion can be significantly increased. All these applications make ultra-low phase noise microwave an attractive research topic.

1.1 Microwave Oscillators

Improvements of microwave oscillators are directly responsible for the generation of signals with higher stability. An unstable oscillator will be source of phase noise in the signal generated. Microwave oscillators come in many different designs but the basic principles are always the same. An oscillator produces an oscillation, that is, a periodic fluctuation about a central point. An electronic oscillator produces an alternating current (AC) of a desired frequency. To increase the power, the AC signal is amplified. Due to energy losses, the oscillation will dampen and the signal will decrease in amplitude. To maintain the signal at the same amplitude, a part of the output is fed back to the oscillatory circuit (Figure 1.1).

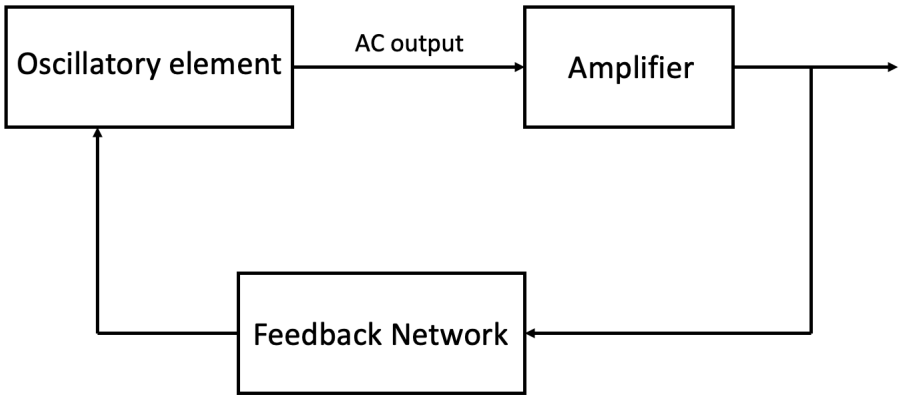

FIGURE 1.1: Block diagram illustrating the three parts of an oscillator. The oscillatory element produces the AC signal, which is then amplified and partially fed back to the oscillatory element to sustain the oscillation.

The most basic oscillatory element is an LC circuit, which consists of a capacitor (C) whose plates are connected to an inductor (L). The oscillation comes from the continuous charging and discharging of the capacitor as the inductor's changing magnetic field forces the cycle to repeat. The circuit is a resonator, the amplitude of the oscillation is higher at the natural frequency of the circuit, called the resonant frequency, that is determined by the geometry of the components. The energy lost to the materials (wires, dielectrics, etc) as heat and from the emission of electromagnetic waves, causes the oscillation to fade away. The quality factor Q quantitatively describes this damping and is defined as the energy stored to the ratio of energy lost per cycle. For an LC circuit the Q-factor is typically on the order of 10^2. According to Leeson's model, the higher the Q-factor of a resonator is, the lower is the phase noise of the signal generated [2]. For widely tunable oscillators the quality factor tends to be limited but can still reach high values. For example, a YIG (yttrium iron garnet) tuned oscillator has a Q-factor typically above 4000 at 10 GHz, offering a good phase noise performance despite its large tuning range [3]. Many electronic resonators were designed to reach higher quality factor values at similar frequencies. A dielectric resonators has a Q-factor of 5000 at 10 GHz [4]. State of the art electronic oscillators, can reach Q-factor of the order of 10^5, an example being sapphire loaded cavity resonators at a 9 GHz resonant frequency [5]. High Q-factor oscillators have enabled the implementation of improved communication systems such as 5G [6]. Electronic resonators are still limited in performance however. The energy loss from dielectrics or from the electrical resistance has led researchers to focus on new types of oscillators.

1.2 Optoelectronic Oscillators

To achieve even higher quality factors, certain resonator design make use of optics to generate microwaves. Optoelectronic oscillators (OEO) for instance use laser light to generate a microwave signal via photo-detection. Figure 1.2 shows a conventional OEO which consists of a laser source, an electro-optical modulator (EOM), an optical delay line, a photodetector, an electrical amplifier, and a bandpass filter. The laser light is converted to a microwave signal by the photodetector. The feedback system

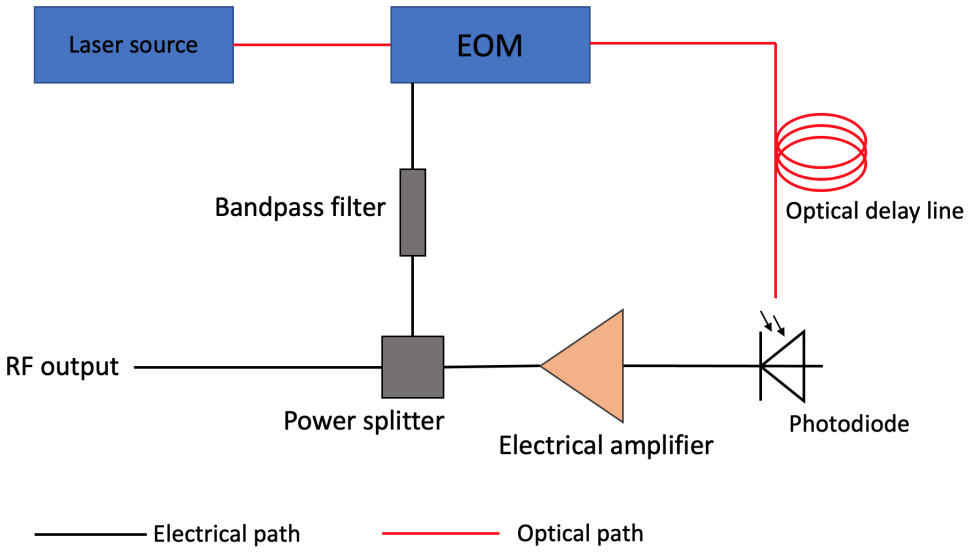

FIGURE 1.2: Schematic of an optoelectronic oscillator. The fiber delay line provides the desired high Q-factor. The feedback goes to the electro-optic modulator (EOM) to sustain the oscillation.

consist of an EOM, which uses a part of the electrical signal to modulate the intensity of the beam and thus sustain the oscillation. The band pass filter allows to select a frequency to obtain the desired oscillation mode. The fiber delay line is used as the energy storage element and its ultra-low loss provides the high quality factor for the system [7]. This basic OEO setup was the first of its kind, many other microwave photonics approaches have followed since. The best phase noise performance to-date has been achieved with mode locked lasers. Mode locked lasers emit periodic trains of ultrashort pulses with extremely precise regularity and at very high pulse repetition frequencies. The stabilized light emitted by a mode locked laser is called an optical frequency comb (OFC). The OFC can be stabilized using an optical cavity. The very high quality factor of an optical cavity ($Q \sim 10^{11}$) allows to lock the frequency of a continuous wave (cw) laser, which is in turn used to lock the OFC. Such a system can be used to obtain ultra-low noise microwaves. However, the setup is complex, expensive and requires an amount of space and power restricting its applications outside of the lab.

In this thesis, the monolithic mode-locked laser (MMLL) will be presented as a practical and simple source of ultra-low noise microwaves, offering an alternative from conventional mode-locked lasers. The MMLL is a compact laser requiring a small amount of power. The high repetition rate of femtosecond (fs) pulses of light generated by the MMLL can be photo-detected to generate ultra-low noise microwaves. The goal of this thesis is to measure the phase noise of a 16 GHz microwave signal generated by a MMLL. This will be done by a direct comparison between the 16 GHz microwave signal and an optical frequency comb locked to an optical cavity. The measurement will demonstrate the use of a cross-correlation technique with two dual output Mach-Zehnder modulators (DO-MZMs) used as phase detectors. We will find that the phase noise of the 16 GHz is comparable to the phase noise of state-of-the-art microwave sources.

Chapter 2

Background Theory

In this chapter, I will explain the concepts that are essential to understand my project. I will define the phase noise of a signal and how it can be measured followed by a description of longitudinal modes are for a resonator and what it means for modes to be phase-locked. Finally, I will explain optical frequency combs and we will understand their usefulness as optical references.

2.1 Phase Noise

Phase noise expresses the frequency instability of a waveform. A monochromatic beam will not be a perfect sinusoidal wave but will deviate from perfect periodicity. One can observe this phenomenon by looking at the power spectral density (the power vs the frequency) of the signal. For a single frequency microwave, one would expect to see a peak located at a given frequency, the "carrier frequency", whose height corresponds to the power of the signal. In reality, the signal is covering a range of different frequencies. The measurement of other frequencies comes from the frequency instability of the microwave beam, jittering around the main frequency called the carrier frequency. Fig 2.1 illustrates the spectral density of a signal whose carrier power is represented by the black line. Phase noise is typically expressed as the power ratio between the carrier to the noise power spectral density (typically expressed as the noise power within 1 Hz), as a function of the offset frequency from the carrier. A phase noise measurement plot typically shows the logarithm of the ratio of the carrier power to the offset powers (in dBc/Hz), as a function of the offset frequency. As an example, a conventional oscillator, such as a frequency multiplied crystal oscillator with a carrier frequency of 9 GHz will

have a phase noise of -110 dBc/Hz at an offset frequency of 1 kHz. In comparison, high performance oscillators, such as a sapphire loaded cavity oscillator, can reach a phase noise of about -140 dBc/Hz at 1 kHz at a carrier frequency of 9 GHz [8]. This is a thousand times better. Figure 2.2 shows the phase noise of those two oscillators for offset frequencies ranging from 100 Hz to 100 kHz.

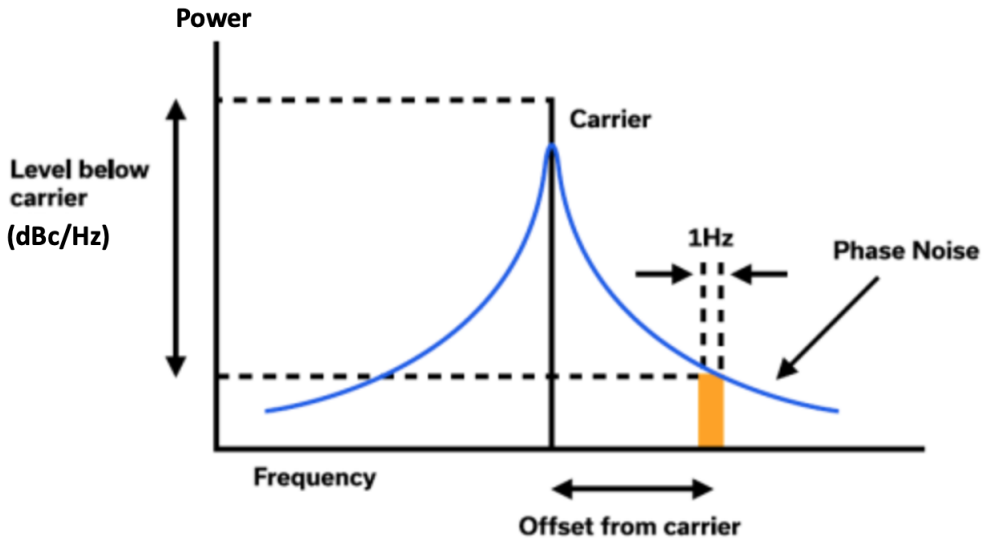

FIGURE 2.1: Power spectral density of a signal whose phase noise is represented by the sidebands in blue. Phase noise is measured at an offset from the carrier in a 1 Hz bandwidth and is expressed as the power ratio between the carrier to the noise power spectral density [9].

Amplitude noise is the other important manifestation of the instability of a signal. Amplitude noise can be a problem when measuring phase noise as amplitude noise can convert to phase noise in circuits. This occurs when the signal undergoes non-linear effects, mostly in amplifiers and photodiodes. Other types of noise are important to consider when making a phase noise measurement. Phase noise can be generated from random noise sources, such as thermal noise, flicker noise and shot noise. Thermal noise is the fluctuation in voltage due to the thermal vibrations of electrons in resistors, inductors and capacitors. An instrument with a high thermal noise will contribute to both the phase noise and the intensity noise of a signal. Thermal noise generally sets the noise floor (lower limit) to a phase noise measurement. Flicker noise is also a type of noise found in instruments but its fundamental origin is often not well understood. Flicker noise is often called 1/f noise because

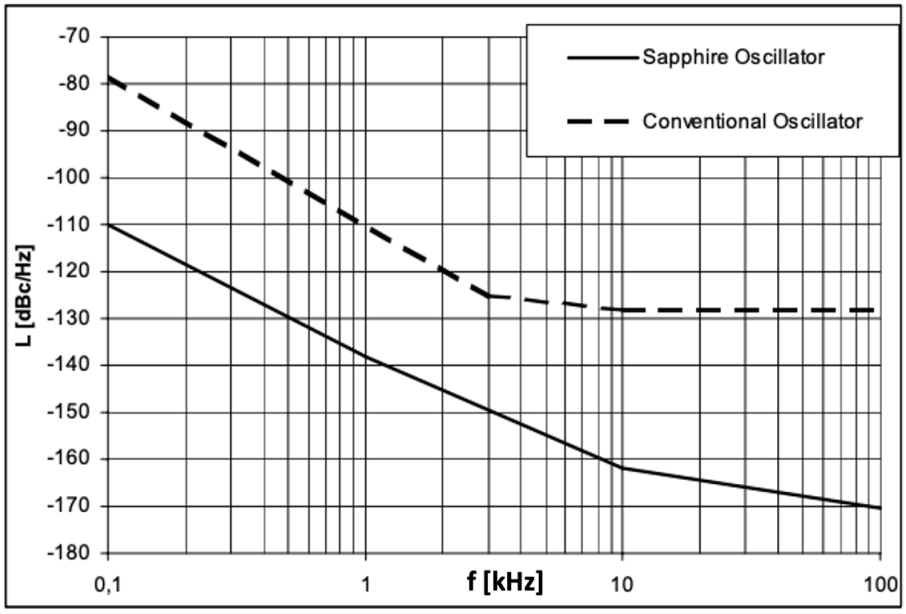

FIGURE 2.2: Plot of the phase noise of two oscillators at 9 GHz, a crystal oscillator and a sapphire loaded cavity oscillator. The sapphire oscillator is a thousand times less noisy than the conventional oscillator [8].

it often manifests a power spectral density as an inverse function of frequency. In oscillators, flicker noise can interact with the resonant frequency and thus can cause frequency instabilities. Shot noise is a noise arising from the discreteness of photons and electrons. The flow of discrete electrons results in small random direct current fluctuations. Shot noise is frequency and temperature independent, unlike thermal and flicker noise. At high frequencies and low temperatures, shot noise may become the dominant source of noise. Shot noise is a fundamental limit to amplitude and phase noise and is important to consider when using photodiodes. The random occurrence of photon absorption in a photodiode leads to current fluctuations.

2.2 Phase Noise Measurement

There exists different approaches to measuring phase noise but the most common ones all rely on the same principle. The idea is to compare our device under test (DUT), i.e. our oscillator, to a reference oscillator whose phase noise is known to be lower. The simplest phase noise measurement method is to input the oscillator signal into a spectrum analyzer. In this case, the reference oscillator is the local oscillator of the spectrum analyzer. The spectrum analyzer measures the carrier power

and the noise signal at offsets from the carrier and then a software function derives the noise power spectral density of the oscillator under test. This method is limited by the noise of the local oscillator and the dynamic range of the spectrum analyzer. Spectrum analyzers often cannot differentiate amplitude noise and phase noise, so one may get an erroneous measurement if the amplitude noise is not significantly lower than the phase noise.

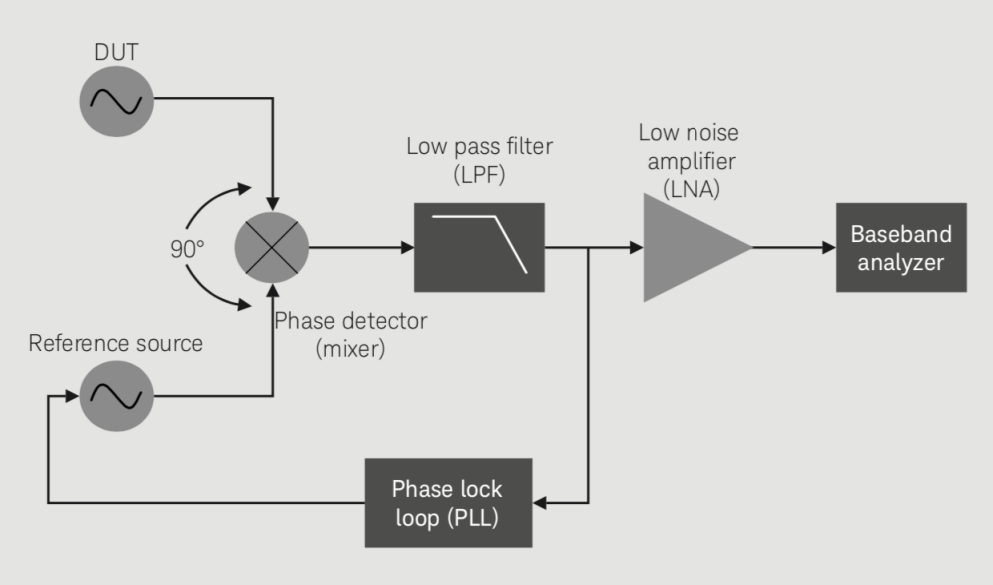

FIGURE 2.3: Block diagram of the quadrature method for the phase noise measurement of an oscillator [10]. The frequency mixer generates the sum and the difference of the two frequencies. The sum frequency is filtered by the low pass filter and the phase lock loop keeps a 90° shift between the signals phase.

To avoid such a problem we use phase detection techniques that are insensitive to amplitude (AM) noise. A phase detector takes two signals with the same frequency but having a 90° phase difference (quadrature) so that their product give a near zero voltage at the output. The phase detector thus converts a small phase difference from quadrature between two signals to a voltage that is approximately proportional to the phase difference between the two oscillators. A schematic of the quadrature method is shown in Figure 2.3. The signal from the reference oscillator and the oscillator under test are combined in a frequency mixer which generates the sum frequency and the difference frequency of the two signals. The mixer sum frequency is filtered by a low pass filter, while the difference frequency is amplified by

a low noise amplifier. The phase locked-loop keeps the phase of the reference signal shifted by 90° to the signal under test. This method will provide a measurement whose sensitivity is limited by noise of the instruments.

The noise inherent to the instruments can be diminished by using the two-channel cross-correlation technique. This technique (shown in Fig 2.4) combines two identical channels and performs the cross-correlation of the two output signals. The noise of the DUT is coherent and is not affected by the cross-correlation. The incoherent noise of the two channels is reduced by a factor of $\sqrt{M}$ where M is the number of correlation measurements averaged. The total measured noise, N_{meas}, can be expressed as:

$$N_{meas} = N_{DUT} + \frac{N_1 + N_2}{\sqrt{M}}$$

where N_1 and N_2 are the noise of channel 1 and 2, respectively. This technique allows a high sensitivity that may be necessary for the measurement of state of the art oscillators. To measure the ultra-low phase noise of a mode locked lasers a cross spectrum technique may be required. In the next section, we will understand mode locking, the principle mode locked lasers are based on.

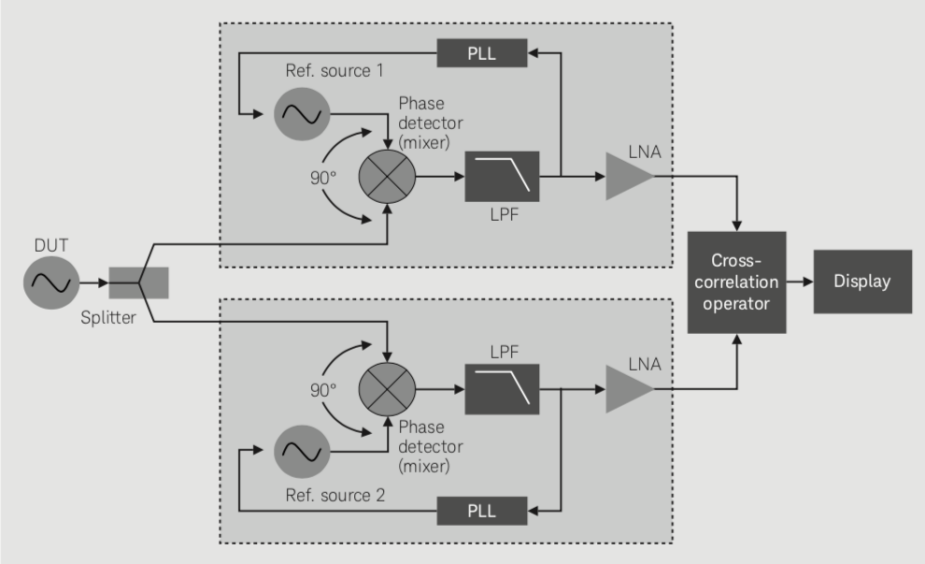

FIGURE 2.4: Block diagram of two-channel cross-correlation technique [10]. The signal from the DUT is split in two identical channels whose noise are uncorrelated. The cross-correlation operator will average out the uncorrelated noise, reducing the noise floor and allowing a higher sensitivity to measure the correlated noise from the DUT.

2.3 Mode Locking

Mode locking is a technique used to generate very short flashes of light from a laser, thus called a mode locked laser. The ultrashort pulses of light typically last a few to a few hundred femtoseconds (10^{-15} s) and are emitted at very regularly spaced intervals, forming sequences called pulse trains. The pulse repetition rate of a pulse train is the number of pulses emitted in, e.g., one second.

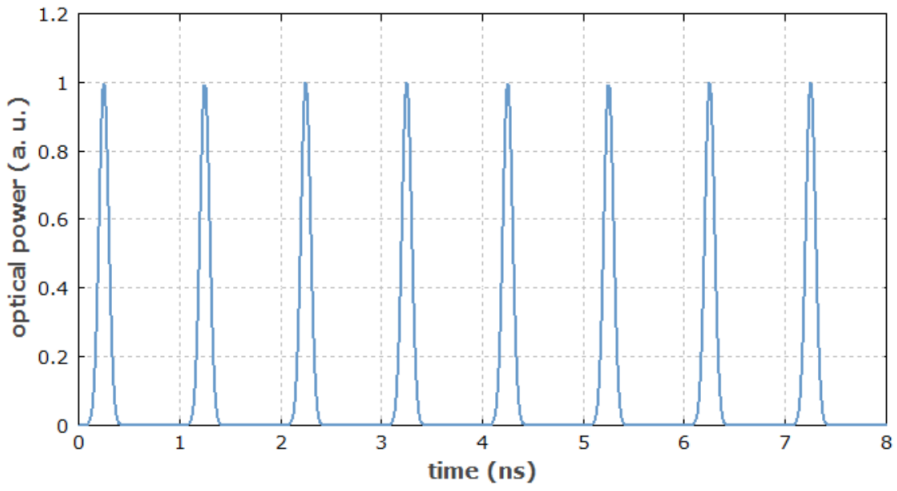

FIGURE 2.5: Regular light pulses emitted every nanosecond [11].

Figure 2.5 shows an example for a repetition rate of 1 GHz, corresponding to a pulse spacing of 1 ns. One needs a mode locking device (mode locker) within the laser cavity to obtain such evenly-spaced short pulses. The cavity modes or longitudinal modes are the electromagnetic standing waves allowed to exist in the laser cavity. The mode spacing is defined by the geometry of the cavity.

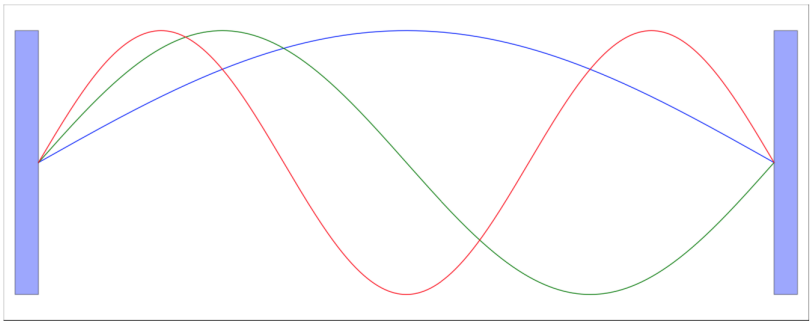

FIGURE 2.6: The first three modes of a cavity [12].

Figure 2.6 shows the first three modes for a cavity of length L. The first mode has a wavelength that is twice the cavity length, i.e. $\lambda_1 = 2L$, the second mode has a wavelength of L, and the third mode $\frac{2L}{3}$, etc. More generally, the wavelength of each mode is given by $\lambda_m = \frac{2L}{m}$, where m is an integer. We can use this formula to find the mode frequencies to be $m\frac{c}{2nL}$, where c is the speed of light in vacuum and n is the index of refraction of the wavelength λ_m. Generally, these modes all have random phases relative to each other and so their resulting interference will be a beam with random intensity fluctuations.

Figure 2.7 shows an example of a beam with a random sequence of pulses. In this example, 31 oscillating modes are separated in frequency by the spacing between two adjacent modes: $\Delta\nu = \frac{c}{2nL}$. Although the mode's random phases will result in a random sequence of pulses, the approximate equidistance between each frequency will lead the random sequence to be repeated periodically at least over short time intervals. The random waveform has the properties of a Fourier series. The waveform frequency is equal to the frequency between adjacent modes ($\Delta\nu = \frac{c}{2nL}$). Each light pulse has a duration roughly equal to $\Delta\tau_p = \frac{1}{31\cdot\Delta\nu}$.

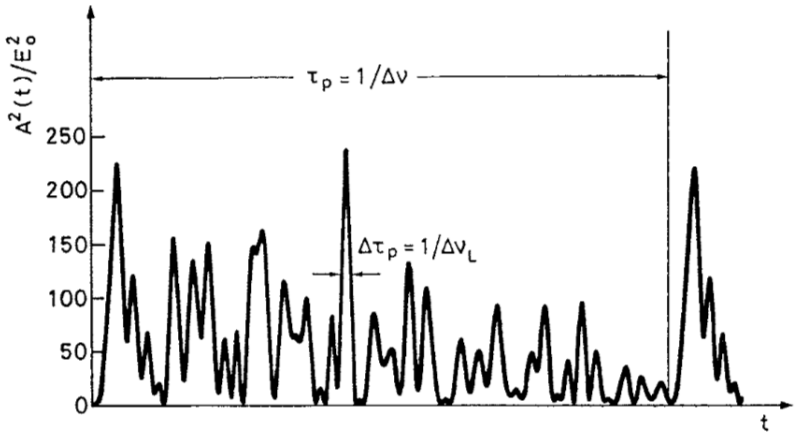

FIGURE 2.7: Intensity fluctuations of a laser light when the modes have random phases [13]

Establishing a definite relation between the phases of the oscillating modes will produce the train of evenly spaced light pulses. If the phases ϕ_l of the modes are locked according to $\phi_l - \phi_{l-1} = \phi$, the electric field can be written as:

$$E(t) = \sum_{l=-n}^{n} E_0 e^{i[(\omega_0 + l\Delta\omega)t + l\phi]}$$

where ω_0 is the angular frequency of the central mode and $\Delta\omega = 2\pi\Delta\nu$ is the angular frequency difference between any two modes [13].

Figure 2.8 shows the case of seven oscillating modes with locked phases. The beam intensity is high for a very short time and then vanishes. The pulse repetition rate is given by $\Delta\nu = \frac{c}{2nL}$, the frequency separation between two consecutive oscillating modes, as before.

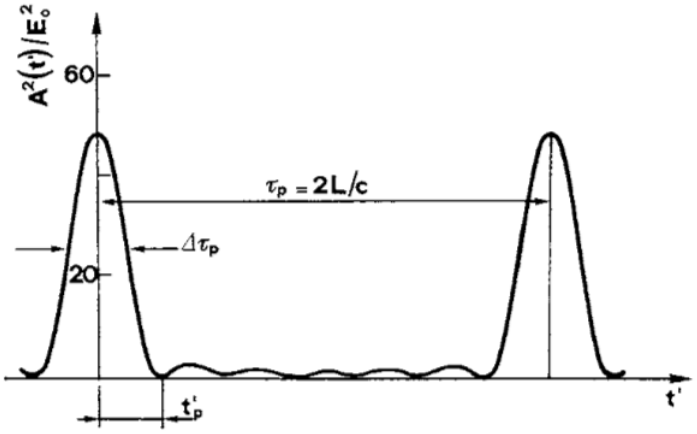

FIGURE 2.8: Pulses of mode locked laser resulting from the phase locking of the modes [13].

2.4 Optical Frequency Combs

An optical frequency comb (OFC) is an optical spectrum for which the optical frequency components are equidistant. The phase relation between the modes is fixed, and as we have seen in the previous section, this can be done with a mode-locked laser. Other methods to generate OFCs include electro-optic frequency combs and Kerr frequency combs [14]. Figure 2.9 shows an OFC, where the power spectral density is plotted as a function of the frequencies of the light. The equidistant lines form a comb-like structure.

This structure arises from a pulse train, a sequence of pulses emitted very regularly, as in a mode locked laser. The time domain picture of an OFC is thus the pulse train picture seen in Figure 2.5. Taking the Fourier transform in the time domain

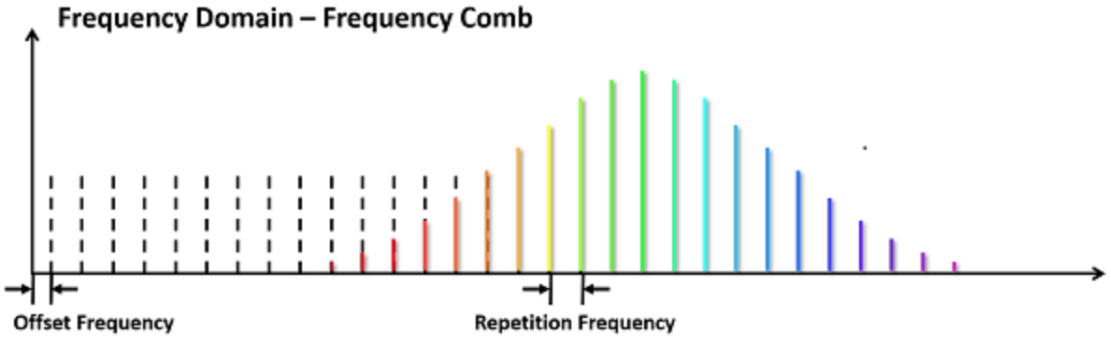

FIGURE 2.9: An optical frequency comb, where each comb line is a frequency of the light and are separated by the repetition frequency [15].

gives the comb picture from Figure 2.9. The frequency separation between each line (comb spacing) is equal to the pulse repetition frequency (f_{rep}). The offset frequency of the first comb line from zero is called the carrier-envelope offset frequency (f_{CEO}). This offset corresponds to a phase shift ($\Delta\phi_{CEO}$) of the electric field's oscillation with respect to the pulse envelope (Figure 2.10). The velocity of the envelope (group velocity) and the velocity of the electric fields' phase (phase velocity) are not always equal because of chromatic dispersion or optical nonlinearities. This velocity difference results in the carrier envelop offset frequency.

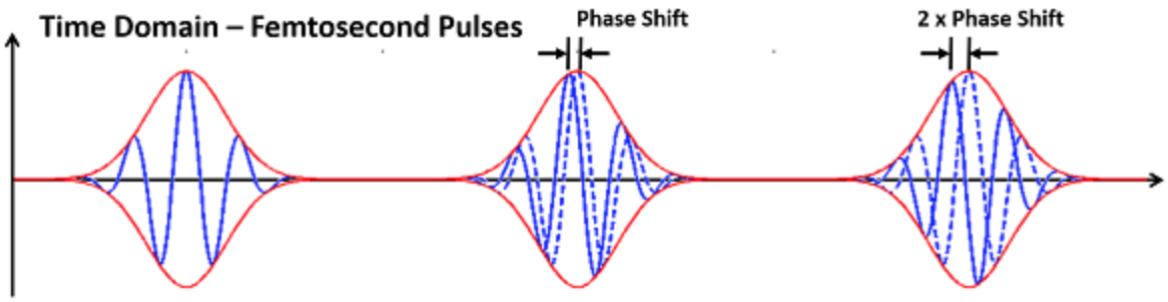

FIGURE 2.10: Phase shift between the pulse envelope and the electric field resulting from the difference between the group velocity and the phase velocity. The carrier-envelope offset frequency is the frequency of the very first comb line [15].

Therefore, to get the optical frequency of the n^{th} longitudinal mode one needs to account for the carrier-envelope frequency:

$$f_n = f_{CEO} + n \cdot f_{rep}$$

where $f_{CEO} = \frac{\Delta\phi_{CEO}}{2\pi} f_{rep}$ [15]. If both f_{CEO} and f_{rep} are known, then all frequencies of

the OFC can be found. The OFC can then be used to measure unknown frequencies within the frequency range (bandwidth) of the comb. This is done by recording a beat note between the unknown frequency and the nearest comb line. A beat note is an oscillation of the optical intensity resulting from the superposition of different optical frequencies. When two laser beams with different optical frequencies are superimposed, a fast intensity photodetector can record the oscillation of power due to this superposition (Fig 2.11). In the case of an OFC, we have many well-defined optical frequencies, and the beat note will originate from the closest comb line to the unknown frequency, which are separated by the lowest beat frequency. The unknown frequency is measured to be above or below the closest comb line by analyzing the changes of the beat frequency as we tune the unknown frequency.

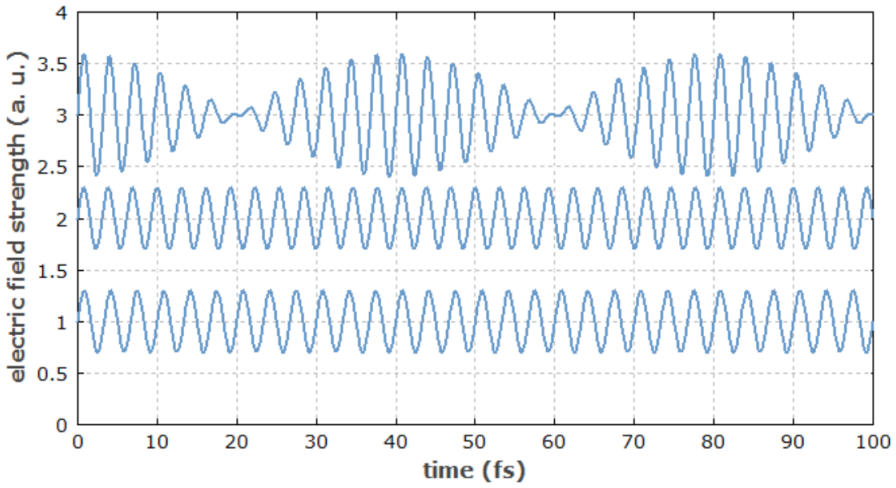

FIGURE 2.11: The top graph shows the beat note resulting from the superposition of the two signals shown at the bottom [16].

OFCs can become highly stable sources when the repetition rate and the carrier-envelope offset are locked to a low-noise RF reference. This low-noise reference can be achieved using a cw laser that is locked to a high finesse cavity, such as a Fabry-Perot cavity. Phase-locking of f_{rep} is done by bringing one of the longitudinal modes of the OFC and the cavity-stabilized laser to interference producing a photo-detected beat note. The beat frequency is tuned by changing the cavity length, which also changes f_{rep}. The f_{rep} locking is achieved when the frequency of the n^{th} comb line is equal to the optical reference frequency. The CEO frequency stabilization requires technical operations outside of the scope of this thesis. Once the OFC is stabilized,

by locking f_{rep} and f_{CEO}, it can be used as ultra-low noise optical reference.

Chapter 3

Experimental Setup

Microwave and radio frequencies are of great importance to modern technology. Our communication systems rely on the generation, distribution, and processing of microwave and radio signals. Ultra-low noise signals have enabled novel approaches to radar technologies, astronomical imaging (using very long baseline interferometry), and high-speed analog-to-digital conversion. The low noise of mode locked lasers has led to new oscillator designs, transferring the high stability of optical pulse trains to microwaves. Such designs are often complex and bulky however, limiting their applications. The motivation for more compact and simpler setups have led to the monolithic mode-locked laser [17]. This low noise laser is used to generate microwaves via photo-detection. The goal of the experimental setup is to measure the phase noise of the microwave using electro-optic sampling techniques and evaluate the performance of the monolithic mode-locked laser as a highly stable microwave source. The measurement will make use of an optical frequency comb as the optical reference and a cross spectrum technique is employed to diminish the uncorrelated noises.

3.1 Monolithic Mode-Locked Laser

The Monolithic Mode-Locked Laser (MMLL) is a mode-locked laser with a cavity made up of one material, calcium fluoride (CaF_2). The MMLL is shown in Fig 3.1. The CaF_2 spacer is about 8.5 cm long and serves as the laser cavity. This medium is desirable for two main reasons. First, CaF_2 has excellent transparency, meaning that very little light is absorbed by the material and thus power losses are low. Second,

CaF_2 has a zero second-order dispersion around 1545 nm, a wavelength corresponding to a frequency close to the center of the comb. Different frequencies will travel at different velocity in a material, resulting in the broadening of light pulses in time (they disperse). This dispersion can be investigated by Taylor expanding the spectral phase of the electric field. The second order dispersion is the second order term of the Taylor expansion, corresponding to the second derivative of spectral phase with respect to angular frequency evaluated at the center frequency. In the MML, the third order dispersion (third derivative of spectral phase) is non zero as opposed to the second order dispersion. To compensate for the third order dispersion and achieve short pulses, a Gires-Tournois interferometer (GTI) coating is deposited on the CaF_2 spacer.

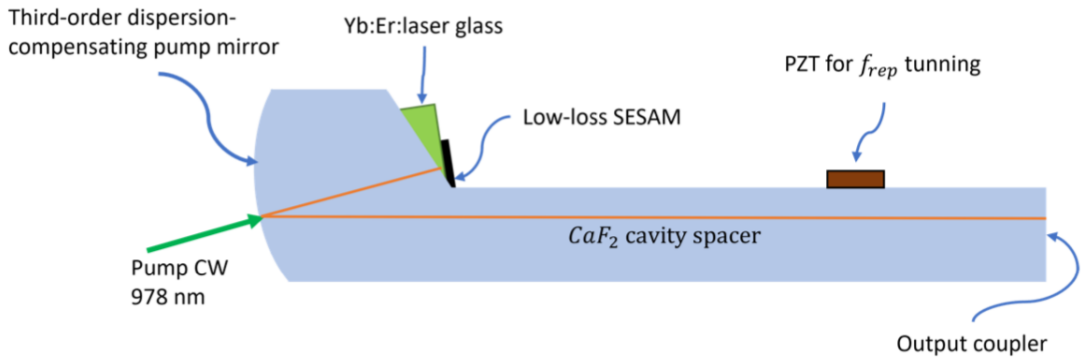

FIGURE 3.1: The Monolithic Mode-Locked Laser [3]

The laser light is amplified through the gain medium, Ytterbium:Erbium:glass. The mode locker is a semiconductor saturable absorber mirror (SESAM) and is attached to the gain medium. The SESAM has low degree of absorption at low intensities. This phenomenon is responsible for the mode locking mechanism as the light pulses reflected on the SESAM are shortened as shown in Fig 3.2 . The SESAM has a saturable loss of about 0.5%, meaning that when the SESAM is not saturated, 0.5% more of the light is lost compared to when the SESAM is saturated. The MMLL has a repetition rate of 1 GHz which can be tuned slightly via temperature control and the piezoelectric transducer that compresses the CaF_2 spacer.

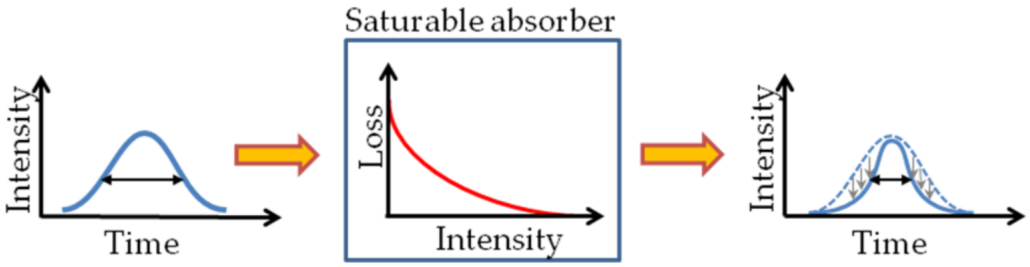

FIGURE 3.2: Effect of a saturable absorber on a light pulse. The low intensity parts of the pulse get absorbed leaving a sharper pulse [12].

3.2 Microwave Generation

To generate microwaves from optical pulse trains, a photodetector is needed. A photodetector can absorb only a certain amount of intensity. If the incident light is too intense, the photodiode saturates, the output current no longer increases as the intensity increases. The photo-detection can thus be improved by dividing the intesnity of the incident light. In the case of an optical pulse-train this can be done by multiplying the pulse repetition rate. In the experiment, the light emitted from the MMLL with a repetition rate of 1 GHz is increased to 16 GHz. This is done with a 4-stage free space pulse inter-leaver (Fig 3.3). This is a four stage inter-leaver, each stage doubles the pulse repetition rate. The light coming from the MMLL is linearly polarized, i.e., the electric field oscillates in one direction only. By going through a half wave plate ($\lambda/2$) the polarization is rotated by an angle chosen. Changing the polarization allows the beam to be split equally by a polarized beam splitter (PBS). Half of the light conserves its direction of propagation, while the other half is reflected by 90° (upward in the figure). Each beam then goes through a quarter wave plates ($\lambda/4$) and gets reflected by highly reflective mirrors. One of the mirrors (top one) is placed further away than the other mirror such that the beams have a time delay of half the pulse interval. The beams go through the quarter wave plates a second time, which has the same effect as going through a half wave plate once. The beams are thus recombined when they get back to the PBS. The transmitted beam is now reflected by 90° (downward in the figure) and the reflected beam is transmitted. The time delay between each beam results in the pulse repetition rate to double. The beam has now a 2 GHz pulse repetition frequency. Each following stage works the

same way: the repetition frequency doubles to 4 GHz, then 8 GHz, and finally to 16 GHz.

The light is now ready to be detected by a photodiode (PD), to transfer the excellent stability from the optical domain to the microwave domain. A photodiode is a semiconductor device with p-n junction or a PIN junction used for the detection of light. The n-region has excess electrons and the p-region has deficit electrons (holes). The intrinsic region is between the n-region and the p-region, and is also a depletion region, where there are no free carriers. When a photon is absorbed by the depletion region, an electron hole pair is generated. Holes move towards the anode and electrons move toward the cathode and a photocurrent is thus produced. The photodiode used in our experiment is called a modified uni-traveling carrier (MUTC) photodiode. In a MUTC-PD, only electrons traverse the depletion region. The MUTC has the important property to be insensitive to amplitude noise for a specific bias voltage. The high speed performance of the MUTC allows to generate the 16 GHz microwave from the MMLL optical pulse trains.

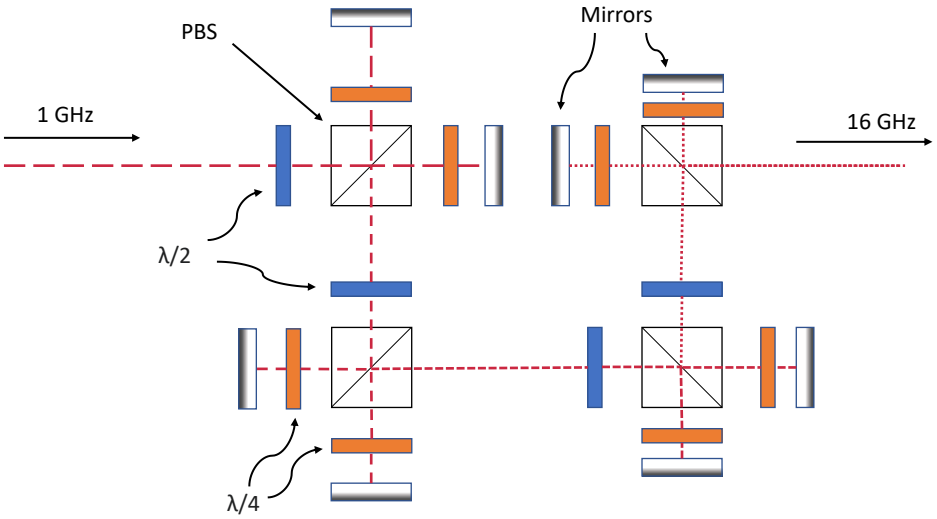

FIGURE 3.3: 4-stage free space pulse interleaver. Each stage doubles the repetition rate by recombining the two beams, one of them having a time delay corresponding to half a pulse separation.

3.3 Microwave Measurement

Measuring the phase noise of the 16 GHz microwave signal requires a complex apparatus. A typical mixer-based phase detector cannot measure such a low phase noise because the noise of signals produced by electronic oscillators is higher than the noise of the signal to be measured. To measure our ultra-low noise microwave, a cross-spectrum method will be used. This method allows to reduce the phase noise by averaging out the shot noise from the balanced photodetectors and the flicker noise of amplifiers. Some phase noise analyzers have the cross-spectrum option, but their acquisition time for the measurement of our microwave is of the order of days. To obtain a sufficiently high sensitivity, we will not use another electronic signal as a reference but an optical pulse train. The high stability of an optical frequency comb allows to improve the sensitivity of our measurement by orders of magnitude. To directly compare the reference OFC with a 500 MHz repetition rate and our 16 GHz microwave a dual-output Mach-Zehnder modulator (DO-MZM) is used as a phase detector (Fig 3.4). The optical reference enters one input of the DO-MZM and takes the two different paths. The two paths recombines after one of the beam interacted with the microwave. The microwave interacts with light in Lithium Niobate, $LiNbO_3$, a crystal that displays the linear electro-optic effect (Pockels effect). The refractive index is changed linearly by the electric field, causing the light to travel slower when an external electric field is applied. The change in phase then results in a change in intensity as the beams recombine at the output beam splitter of the Mach-Zehnder interferometer. One of the output beams will have lower intensity, resulting in a lower photocurrent. The photo-detected currents are subtracted, then converted to a voltage by a trans-impedance amplifier (TIA).

This voltage is related to the phase difference between the microwave and the reference light via a Bessel function. When the microwave and the optical pulse-train are in quadrature, the electric field is be momentarily zero and has no effect on the light, the output voltage is thus zero. If the microwave manifests some phase noise, the pulse will be affected by the electric field, and we will detect an output voltage. Figure 3.5 shows the relationship between the output voltage from the trans-impedance amplifier and the phase error between the microwave and the light.

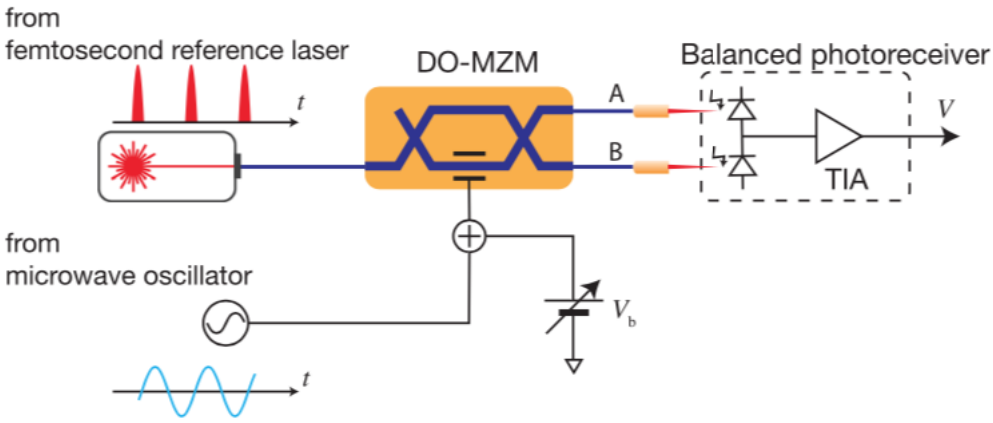

FIGURE 3.4: DO-MZM used as a phase detector [18]. The reference OFC follows two paths, one of which goes through $LiNbO_3$ and interacts with the microwave. A phase fluctuation of the microwave results in output beams with different intensities.

Close to zero, this discrimination signal is well approximated by a linear function. The phase detection just described is subject to the flicker noise of the DO-MZM and the shot noise of the balanced photo-receivers. To overcome these limitations we will add an identical channel, using a second DO-MZM, and perform a cross-correlation of the two signals. The cross-correlation allows to suppress the uncorrelated noises. The phase noise of the microwave through each channel are coherent an are not affected by the cross-correlation. Fig 3.6 shows the complete set up for the microwave phase noise measurement. The MMLL emits ultra short pulses of light at a 1 GHz repetition rate. About 2% of this light is redirected to measure the relative intensity noise of the MMLL using a photodiode. A loop filter feeds the RIN back to the MML to suppress its intensity noise. The remaining of the light is amplified by an erbium doped fiber amplifier (EDFA) and then goes through the inter-leavers to multiply the repetition rate from 1 GHz to 16 GHz. The optical pulse trains are detected by the MUTC, generating the 16 GHz microwave. A bandpass filter is used the filter out the harmonics. The 16 GHz microwave is split in two by a power splitter, then each part is amplified by RF amplifiers before entering the DO-MZMs. Isolators (ISO) are used to remove the signals reflected off the amplifiers. A phase shifter allows to adjust the phase difference between channel 1 and channel 2. The balanced photocurrents are amplified by trans-impedance amplifiers (TIA) and low noise amplifiers (LNA). The cavity-locked reference OFC is also divided in two parts, one for each channel. To

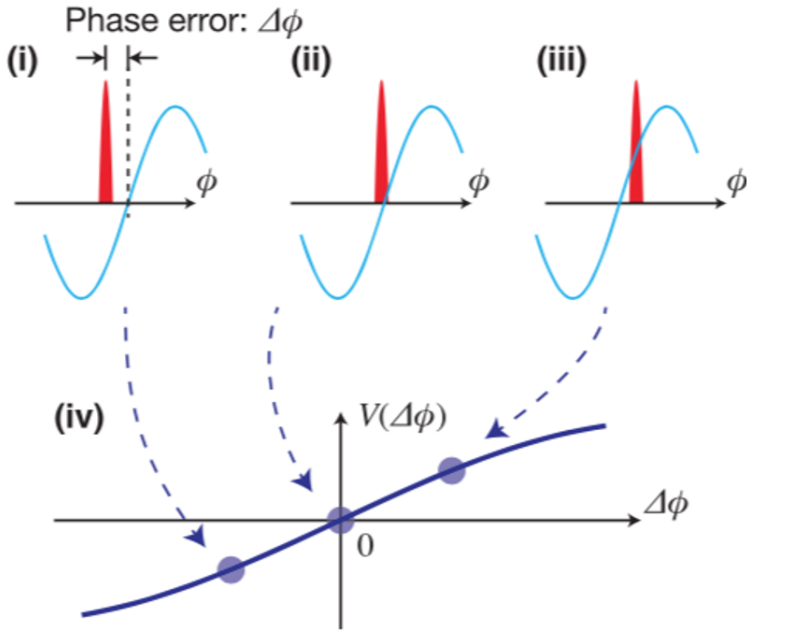

FIGURE 3.5: Voltage signal as a function of microwave phase noise [18]

obtain quadrature between the 500 MHz OFC and the 16 GHz microwave, the microwave frequency is match to the 32nd harmonic of the OFC. This is achieved with a slow feedback loop, using the the trans-impedance output as the error signal to be fed back to the MMLL.

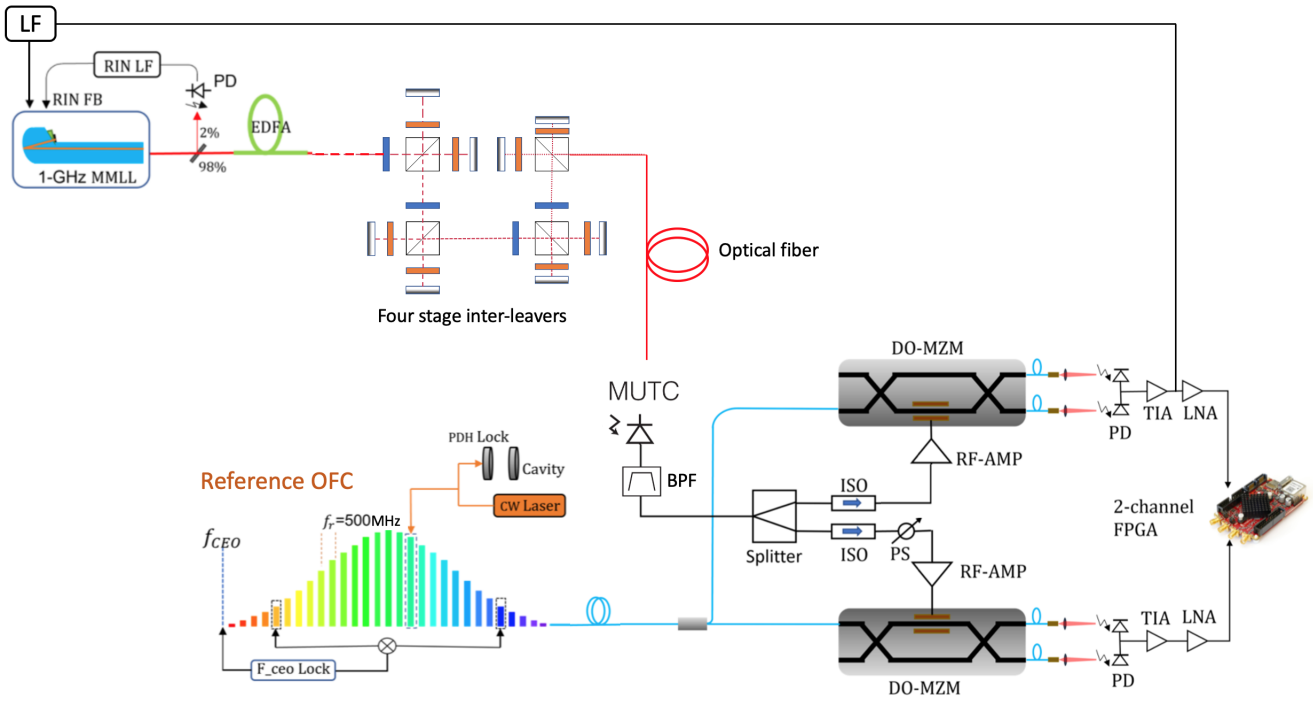

FIGURE 3.6: Microwave phase noise measurement setup with a cross correlation technique using two dual output Mach-Zehnder modulators (DO-MZMs). The reference optical frequency comb (OFC) is locked to an optical cavity. MUTC: modified uni-traveling carrier, RIN LF: relative intensity noise loop filter, EDFA: erbium doped fiber amplifier, BPF: bandpass filter, PD: photodiode, ISO: isolator, PS: phase shifter, RF-AMP: radio frequency amplifier, TIA: trans-impedance amplifier, LNA: low noise amplifier [3].

Chapter 4

Results

In this chapter, I will present the collaborative work that I was part of during this year in the Schibli Lab. I will present the phase noise data of the 16 GHz microwave source and compare it to the phase noise of other oscillators, including a YIG oscillator. But first, I will give a brief overview of some of the preliminary work done: the alignment of inter-leavers, the design of a PI controller, and the MUTC testing.

4.1 Preliminary Work

4.1.1 Adjustment of the Optical Pulse Inter-leaver

To obtain the maximum optical power from the MMLL, it is essential to properly align the pulse inter-leavers described in Chapter 3. The RF spectrum of the microwave signal can be obtain by recording beat notes between the microwave signal and the OFC using the measurement set up (Fig 3.6). The goal of optimization process is to minimize the power of the unwanted sub-harmonics. By blocking the light at certain stages of the inter-leavers, the RF spectrum shows certain harmonics with a higher power. For example, blocking one of the mirrors for each of the last three stages, gives a 2 GHz signal, with an optical spectrum where harmonics multiples of 2 (2 GHz, 4 G Hz, 6 GHz, ...) have a high power. By adjusting the mirrors and the wave-plates to improve fiber coupling, we observe the lowering of odd harmonics. Repeating this process for all four-stages results in the maximized power at the desired 16 GHz carrier, while minimizing the power in all unwanted sub-harmonics. Fig 4.1 shows the RF spectrum of the microwave signal after the realignment of the

inter-leavers. The power of the carrier is 40 dB higher than the power of the unwanted sub-harmonics. This means that about 99.8% of the power is in the desired carrier frequency.

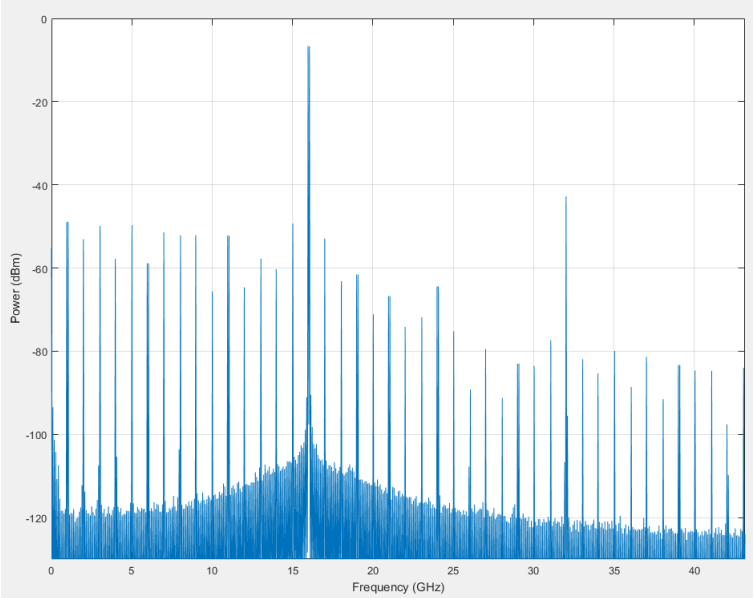

FIGURE 4.1: RF spectrum of the 16 GHz microwave obtained from the measurement setup after realigning the four-stage pule inter-leavers. We observe a suppression of 40 dB.

4.1.2 Construction of the PI Servo-controller

A PI controller is a feedback circuit allowing to continuously correct a parameter of our system. PI controllers are made of a proportional gain and an integral gain. In the microwave experiment, the MMLL needs to be locked to the reference comb to match the microwave frequency to the 32^{nd} harmonic of the 500 MHz OFC. This is done using a slow feedback loop whose error signal was taken to be the voltage output of the balanced photodetectors shown in Fig 3.4. Fig 4.2 shows the circuit designed to obtain quadrature between the comb and the microwave. The proportional gain produces a proportional response to the error signal, while the integrator gain integrates the error over time.

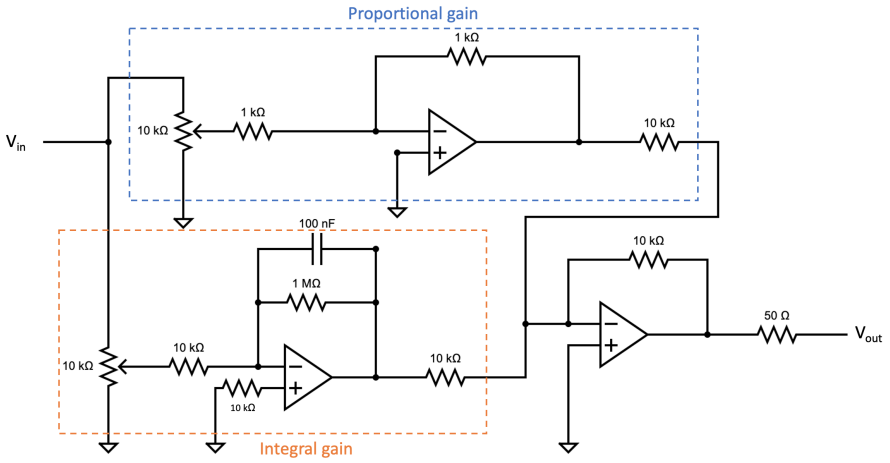

FIGURE 4.2: Circuit diagram of the PID controller used for the feedback loop to lock the microwave to the 32^{nd} harmonic of the reference comb. The input voltage is the trans-impedance voltage from the balanced photo-detection. The output voltage allows to correct the pump power for the MMLL.

4.1.3 Testing the MUTC

To test the MUTC, we have measured its photocurrent and the power of the microwave for different currents for the fiber amplifier (shown in Fig 3.6) corresponding to different optical powers of the pulse train. The data taken is found in table 4.1. The data-sheet of the MUTC [19] indicated a responsivity of 0.4 A/W. As we measured the optical power before the fiber coupling, we have to consider the coupling efficiency. We measured a 12.3 mW of light entering the fiber and 6.9 mW coming out from the other end, which is normally connected to another fiber going to the MUTC. From these values we find a coupling efficiency of 0.56. We can now use our data to find the responsivity of our MUTC by diving the photocurrent by 56% of the optical power from table 4.1. This yields an average responsivity of 0.41 A/W, matching the description of the data-sheet. To further compare our measurement with that of the data-sheet, the RF output power is plotted as a function of the photocurrent in Fig 4.3. The data collected is plotted on the left and corresponds to the data-sheet plot on the right, specifically the lower left region defined by the blue dashed lines.

TABLE 4.1: We measured the input optical power, the RF power, and the average photocurrent of the MUTC for 8 different pump currents of the fiber amplifier.

Pump current (A)	Optical power (mW)	Microwave power (dBm)	Photocurrent (mA)
0.17	3.0	-26.6	0.68
0.27	12.4	-13.33	2.60
0.37	17.0	-8.0	4.80
0.47	32.3	-4.4	7.10
0.57	41.0	-1.92	9.16
0.67	50.0	0.2	11.40
0.77	58.5	1.7	13.30
0.87	68.0	3.0	15.20

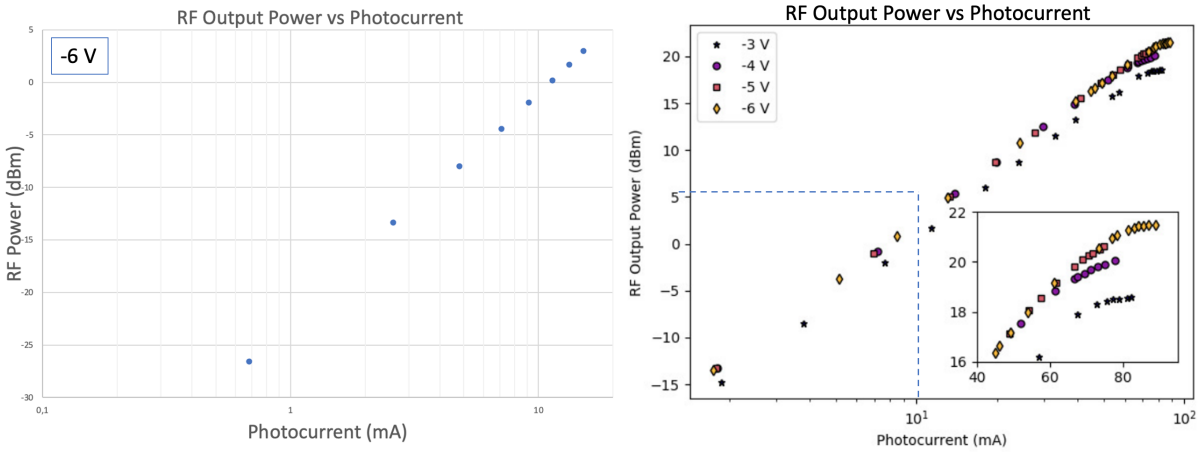

FIGURE 4.3: Comparison between our data for the MUTC output RF power as a function of the photocurrent with the MUTC data-sheet plot [19]. On the left, the data from table 4.1 of the RF power as a function of the photocurrent on a log scale.

4.2 Phase Noise of the 16 GHz Microwave

Using the set up described in section 3.3, we were able to measure the phase noise of the 16 GHz microwave generated by the MMLL. Figure 4.4 shows the plot of the phase noise from the data collected. The phase noise, L(f), in units of dBc/Hz, is plotted as a function of the offset frequency, in Hz. We made two measurements, one using the RIN feedback (shown in Fig 3.6) to suppress the intensity noise of the MMLL, and one without it. We see that the RIN suppression lowers the measured phase noise at low offset frequencies, indicating that the intensity noise of the MMLL does not manifest itself at high offset frequencies. Above 50 kHz offsets, the two curves overlap. At offsets lower than 10 kHz, the RIN suppression improves the phase noise by 5 to 10 dB compared to the phase noise without RIN suppression.

The phase noise of the 16 GHz microwave with RIN suppression reaches about -129 dBc/Hz at a 1 kHz offset, -150 dBc/Hz at 10 kHz, and -164 dBc/Hz at 100 kHz. The number of averages in the cross-correlation measurement was 5.7k below 10 kHz, 92k between 10 kHz and a 100 kHz, and 1.8 million above 100 kHz.

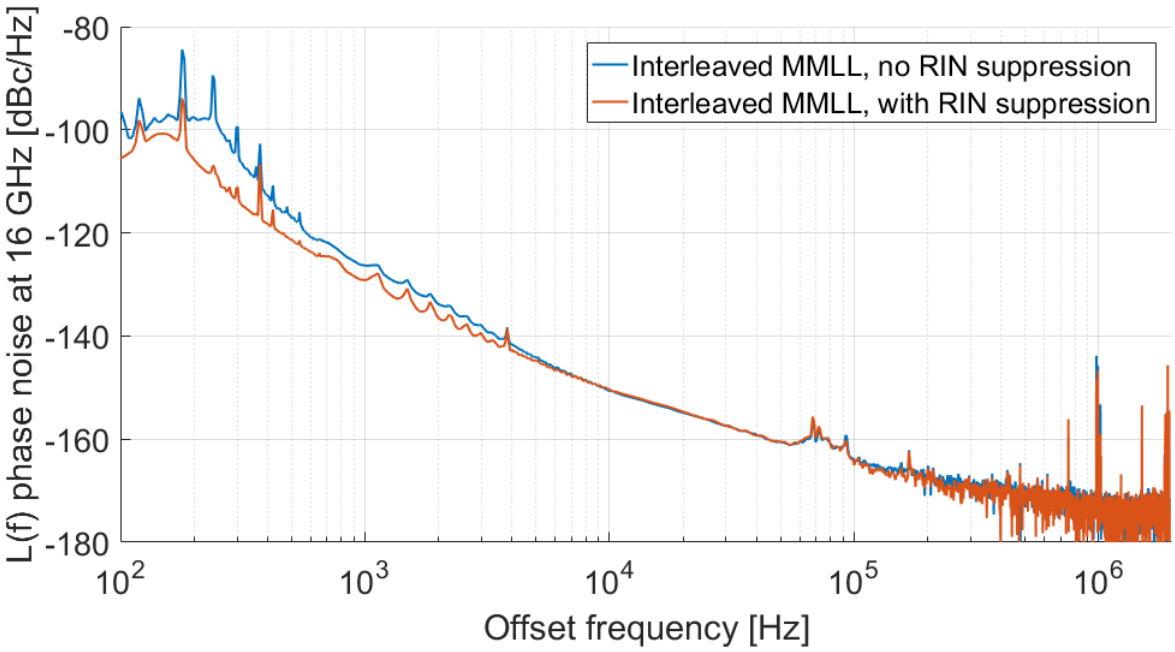

FIGURE 4.4: Measured phase noise of the 16-GHz microwave with RIN suppression in orange and without RIN suppression in blue.

This measurement is somewhat unsatisfying considering the potential of the MMLL. For a 1 GHz carrier frequency, the phase noise was estimated [14] to be -160 dBc/Hz at 1 kHz, -191 dBc/Hz at 10 kHz, and -213 dBc/Hz at 100 kHz. This prediction was confirmed in 2020 [20], with -150 dBc/Hz at 1 kHz, and -167 dBc/Hz at 10 kHz offsets for a 8 GHz carrier. For a 16 GHz carrier frequency, we can use the fact that phase noise is inversely proportional to the square of the ratio between a higher carrier frequency to a lower carrier frequency to shift the above values by $20\log\left(\frac{16\text{ GHz}}{8\text{ GHz}}\right) \approx 6$ dB. We find a theoretical phase noise of -144 dBc/Hz, and -161 dBc/Hz for the same respective offset frequencies. Our measured phase noise is thus about 10 to 15 dB higher than expected. This is most likely explained by an error in the measurement. The bias voltage of the DO-MZMs was observed to drift from its desired value on multiple occasions. The bias voltage of the DO-MZMs ensures

equally intense output beams for the balanced photo-detection. An inappropriate bias voltage results in a phase to intensity noise conversion. This is evidently troublesome because the phase detection is based off an intensity difference assumed to come from a phase difference only. If the bias voltage contributes to the intensity difference, an erroneous measurement will result. Considering this possibility, we can conclude that our measurement of the phase noise of the 16 GHz microwave signal is not its true phase noise, but is most likely about 10 to 15 dB higher. Preventing the bias voltage of the DO-MZMs from the drifting is tricky. We attempted more measurements in the hope to improve the results but they were inconclusive. Soon after, the MUTC was found to be burnt following a power outage. The data presented in table 4.1 corresponds to the testing of a new MUTC acquired in February. The phase noise measurement setup is currently being renewed.

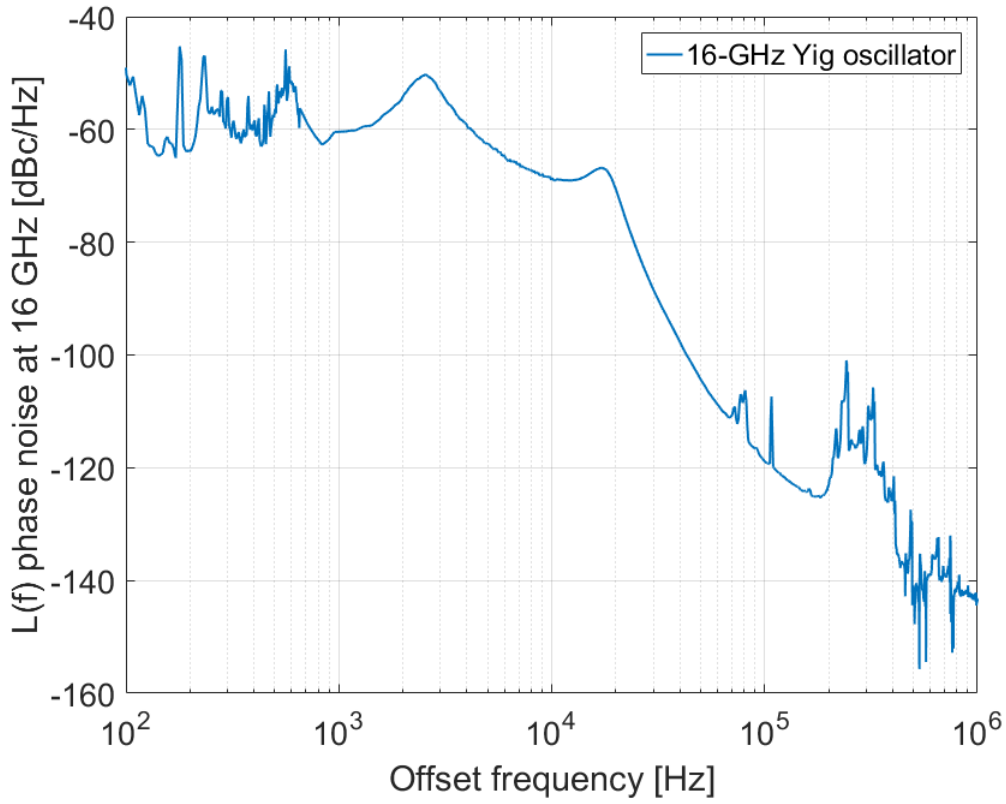

FIGURE 4.5: Phase noise of a YIG oscillator for a carrier frequency of 16 GHz.

To compare our data at the same carrier frequency for a common oscillator we measured the phase noise of a YIG oscillator. This was done using our measurement setup, by replacing the output of the MUTC by the YIG output. Figure 4.5 shows the

plot of the YIG oscillator's phase noise at 16 GHz. The data shows a phase noise of roughly -60 dBc/Hz at a 1 kHz offset, -69 dBc/Hz at 10 kHz, and -119 dBc/Hz at 100 kHz. Comparing the noise performance for each offset frequency between the YIG and the MMLL shows the far superior performance of the MMLL: the phase noise is 8 million times lower, 126 million times lower, and 300 thousand-times lower respectively at 1 kHz, 10 kHz, and 100 kHz offsets, respectively. Due to dielectric losses, YIG oscillators are quite noisy compared to state-of-the-art portable oscillators. To get a more relevant comparison, let's consider the phase noise of an industry standard sapphire loaded cavity oscillator (SLCO) and a photonics microwave oscillator (PMO), which similarly to the MMLL, are compact, portable oscillators. In study conducted in 2019 [21], for a carrier frequency of 3 GHz, the SLCO was reported to have a phase noise of -149 dBc/Hz, -161 dBc/Hz, and -168 dBc/Hz at 1 kHz, 10 kHz, and 100 kHz offsets respectively. This phase noise can be approximated for a carrier frequency of 16 GHz by adding $20\log\left(\frac{16\text{ GHz}}{3\text{ GHz}}\right) \approx 14.5$ dB. This corresponds to -134.5 dBc/Hz, -146.5 dBc/Hz, and -153.5 dBc/Hz for 1 kHz, 10 kHz, and 100 kHz offsets respectively. For the same offset frequencies, the phase noise for the PMO was measured to be -143 dBc/Hz, -152dBc/Hz, and -155 dBc/Hz. We notice that our phase noise data for the MMLL at 1 kHz is higher by 5.5 dB for the SLCO and by 14 dB for the PMO. At higher offsets, the phase noise of the MMLL achieves a better performance however. At a 100 kHz offsets the MMLL has a phase noise lower by 10.5 dB and 9 dB compared to the SLCO and the PMO respectively. Therefore, although our phase noise measurement is higher that expected, it is still comparable to other ultra-low phase noise oscillators of compact size.

In 2017, a fiber based frequency comb generated a 12 GHz microwave with a phase noise below -173 dB/Hz above 10 kHz offsets [22]. Our measured values of -150 dBc/Hz at 10 kHz indicates that our MMLL measurement was still about 100 times noisier (at 10 kHz) than the best low noise lasers. Considering the measurement artifact described above, the theoretical noise of -161 dBc/Hz at 10 kHz for the 16 GHz microwave generated by the MMLL is ten times noisier than the noise of the fiber based frequency comb. At higher offsets, the MMLL even reaches phase noise levels similar to the fiber based comb [20]. We conclude that the 16 GHz microwave generated by the MMLL achieves a phase noise comparable to other highly stable

oscillators, yet the experimental setup used in this thesis encountered difficulties to measure the expected phase noise values mostly due to a failure to stabilize the bias voltage of the DO-MZMs.

Chapter 5

Conclusion and Outlook

The monolithic mode-locked laser (MMLL) can reach phase noise levels comparable to state-of-the art mode-locked lasers. These highly stable mode-locked lasers require complex optical setups whose size and power consumption restrict their applications. The MMLL offers a compact design with a significantly lower power consumption. The generation of ultra-low phase noise microwaves from the MMLL has the potential to improve radar systems, astronomy imaging, and wireless communication. In this thesis, the MMLL was used to generate a 16 GHz microwave signal with ultra-low phase noise. The goal of the project was to measure a phase noise which competes with the best microwave sources. An optical frequency comb (OFC) locked to an optical cavity was used as the phase noise reference. The 16 GHz microwave and the OFC were compared with a dual-output Mach-Zehnder modulator (DO-MZM). The setup included two identical channels to perform a cross-spectrum technique to suppress the noise from the measurement. For the 16 GHz microwave, we measured a phase noise about 10-15 dB higher than expected. This discrepancy was most likely due to the instability of the bias voltage of the DO-MZMs which resulted in an amplitude to phase noise modulation. This measurement still showed a phase noise comparable to ultra-low commercial phase noise oscillators of compact sizes.

The future goal of the experiment would be to improve the measurement setup. One key factor of the measurement quality is the stability of the DO-MZMs bias voltage. New setups are currently being explored to lock this bias voltage. The improved measurement setup will potentially be used to measure the phase noise of a 16 GHz microwave generated by a new micro-resonator design consisting of a 5 mm

wide chip. Such micro-combs made of silicon nitride (Si_3N_4) can reach -80 dBc/Hz at a 1 kHz offset, -110 dBc/Hz at 10 kHz, and -130 dBc/Hz at 100 kHz [23]. Although this phase noise is higher than the MMLL by orders of magnitude, it still provides phase noise levels comparable to modern electronic microwave oscillators. With future improvements in phase noise performance, micro-combs could be integrated to new radar systems and information-processing networks. The continuous progress in microwave photonics will soon allow new oscillator designs to reach ever-increasing phase noise performances.

Bibliography

[1] Gian Carlo Corazza. Marconi's history [radiocommunication]. *Proceedings of the IEEE*, 86(7):1307–1311, 1998.

[2] Karim Benmessaı, Nicolas Bazin, Pierre-Yves Bourgeois, Yann Kersalé, Vincent Giordano, Michael E Tobar, John G Hartnett, Giuseppe Marra, and Mark Oxborrow. Solution looking for a problem: The fe3+: sapphire whispering-gallery-mode 12.04 ghz maser oscillator, an x-band microwave source of extremely low phase noise. In *Meeting of the ARMMS RF and Microwave Society*, pages http–212, 2008.

[3] Manoj. P. Kalubvilage. *Photonic Microwave Generation with Free-running Monolithic Optical Frequency Combs*. PhD thesis, University of Colorado Boulder, 2022.

[4] Nor Muzlifah Mahyuddin, Mohd Fadzil Ain, Syed Idris Syed Hassan, and Mandeep Singh. A 10ghz phemt dielectric resonator oscillator. In *2006 International RF and Microwave Conference*, pages 26–30. IEEE, 2006.

[5] JG Hartnett, ME Tobar, D Cros, J Krupka, and P Guillon. Exceptionally-enhanced q-factor sapphire-loaded-cavity te/sub 01/spl delta//mode resonators. In *Proceedings of the 2002 IEEE International Frequency Control Symposium and PDA Exhibition (Cat. No. 02CH37234)*, pages 559–564. IEEE, 2002.

[6] Fang Zou, Lei Zou, Bo Yang, Qian Ma, Xihua Zou, Jim Zou, Siming Chen, Dusan Milosevic, Zizheng Cao, and Huiyun Liu. Optoelectronic oscillator for 5g wireless networks and beyond. *Journal of Physics D: Applied Physics*, 54(42):423002, 2021.

[7] Ming Li, Tengfei Hao, Wei Li, and Yitang Dai. Tutorial on optoelectronic oscillators. *APL Photonics*, 6(6):061101, 2021.

[8] T Wallin, L Josefsson, and B Lofter. Phase noise performance of sapphire microwave oscillators in airborne radar systems. In *GigaHertz 2003. Proceedings from the Seventh Symposium*, number 008. Linköping University Electronic Press, 2003.

[9] Mini-Circuits. Additive phase noise in amplifiers, April 2021.

[10] Keysight Technologies. *Phase Noise Measurement Solutions*, January 2018.

[11] Dr. Rüdiger Paschotta. Pulse trains. *RP Photonics*, May 2022.

[12] Jonah Maxwell Miller. Optimizing and applying graphene as a saturable absorber for generating ultrashort pulses. Undergraduate thesis, 2011.

[13] Orazio Svelto. *Principles of Lasers*, chapter 8. Springer, fifth edition, 2010.

[14] Mamoru Endo, Tyko D Shoji, and Thomas R Schibli. Ultralow noise optical frequency combs. *IEEE Journal of Selected Topics in Quantum Electronics*, 24(5):1–13, 2018.

[15] Caltech. Optical frequency division. *Vahala Research Group*.

[16] Dr. Rüdiger Paschotta. Beat note. *RP Photonics*, December 2022.

[17] Tyko D Shoji, Wanyan Xie, Kevin L Silverman, Ari Feldman, Todd Harvey, Richard P Mirin, and Thomas R Schibli. Ultra-low-noise monolithic mode-locked solid-state laser. *Optica*, 3(9):995–998, 2016.

[18] Mamoru Endo, Tyko D Shoji, and Thomas R Schibli. High-sensitivity optical to microwave comparison with dual-output mach-zehnder modulators. *Scientific reports*, 8(1):4388, 2018.

[19] Freedom Photonics, 41 Aero Camino, Santa Barbara, CA 93117. *FP1015b 35 GHz High-Power Photodetector*.

[20] Manoj Kalubovilage, Mamoru Endo, and Thomas R Schibli. Ultra-low phase noise microwave generation with a free-running monolithic femtosecond laser. *Optics Express*, 28(17):25400–25409, 2020.

[21] Justin W Zobel, Michele Giunta, Andrew J Goers, Robert L Schmid, Jason Reeves, Ronald Holzwarth, Eric J Adles, and Michael L Dennis. Comparison of optical frequency comb and sapphire loaded cavity microwave oscillators. *IEEE Photonics Technology Letters*, 31(16):1323–1326, 2019.

[22] Xiaopeng Xie, Romain Bouchand, Daniele Nicolodi, Michele Giunta, Wolfgang Hänsel, Matthias Lezius, Abhay Joshi, Shubhashish Datta, Christophe Alexandre, Michel Lours, et al. Photonic microwave signals with zeptosecond-level absolute timing noise. *nature photonics*, 11(1):44–47, 2017.

[23] Junqiu Liu, Erwan Lucas, Arslan S Raja, Jijun He, Johann Riemensberger, Rui Ning Wang, Maxim Karpov, Hairun Guo, Romain Bouchand, and Tobias J Kippenberg. Photonic microwave generation in the x-and k-band using integrated soliton microcombs. *Nature Photonics*, 14(8):486–491, 2020.